Young Stellar Populations in the Local Group: an HST and GALEX comprehensive study

L. Bianchi • Y.B. Kang • B. Efremova, D.Thilker • P. Hodge • P. Massey • K. Olsen

Abstract The study of the stellar constituents of star-forming sites in a wide variety of conditions yields the key to interpreting wide-field UV−optical imaging of extended nearby galaxies, and of distant galaxies. We obtained six-band imaging (from far-UV to I) with HST-WFPC2 of 67 sites of recent star formation in eight Local Group galaxies. HST pointings were selected from GALEX wide-field FUV imaging, which traces the young stellar populations. The HST observations were optimized to characterize the hottest, most massive stars in these regions. From the HST photometry, analyzed with stellar model colors, we derived the physical parameters of the massive stars in each field, and of the extinction by interstellar dust. The HST results are used to interpret GALEX UV measurements of SF across the entire galaxies. Our comprehensive photometric study at HST resolution (sub-pc scale in these galaxies) also provides an ideal selection of targets for follow-up spectroscopy with large ground-based telescopes, and in the UV with HST- or WSO-class telescopes, to clarify the influence of metallicity on the properties and the evolution of massive stars.

L. Bianchi

Dept. of Physics & Astronomy, The Johns Hopkins University, Baltimore, MD, USA; bianchi@pha.jhu.edu

Y.B. Kang

Chungnam Nat. Univ., Dept. of Astronomy & Space Science, Republic of Korea

B. Efremova, D.Thilker

The Johns Hopkins University, Dept. of Physics & Astronomy, Baltimore, MD, USA

P. Hodge

Univ. of WA, Seattle, USA

P. Massey

Lowell Obs., AZ, USA

K. Olsen

KPNO, AZ, USA

Keywords stars: massive ; stars: early-type; stars: evolution ; stars: formation; ultraviolet: stars; galaxies: stellar content ; galaxies: star formation; (galaxies:) Local Group ; galaxies: star clusters

1 Introduction. Young Stellar Populations in Local Group Galaxies

The Local Group (LG) of galaxies is an ideal laboratory to study star formation (SF) and stellar evolution in a variety of physical environments, such as galaxy type, metallicity (spanning a factor of $\sim$20), gas density, interactions, and star-formation history (SFH). These galaxies are close enough that individual stars can be resolved with HST imagers, and can be observed spectroscopically with large ground-based telescopes and HST spectrographs. However, ground-based photometric surveys provide limited sensitivity to discern the hottest stars against the background of the overall stellar populations accumulated during the SFH of the galaxy (see Bianchi, 2011). Wide-field UV imaging from GALEX offers great sensitivity to unambiguously trace the presence of hot stars, hence the sites of recent star formation, over the whole extent of large galaxies. Figure 1 shows optical and UV imaging of six gas-rich, star-forming dwarfs in the LG; see Kang et al. (2009) and Bianchi (2011) for UV imaging of M31.

In this paper we describe an ongoing program aimed at a comprehensive detection and characterization of sites of recent star formation in Local Group galaxies from GALEX imaging, complemented by resolved stellar photometry (ground-based and HST) to derive properties of extinction and massive star content of the SF regions, and ultimately by spectroscopy to derive physical parameters of selected subsamples for validating the comprehensive photometric studies. In particular, an HST treasury program (HST-11079, Bianchi PI)

Table 1 The sample galaxies

Galaxy	Distance [kpc]	Type	D_{25} [arcmin]	V [mag]	$E_{(B-V)}$ foreground[a] [mag]
Phoenix	445 $\pm$ 3	dIrr/dSph	4.9 x 4.1	13.1	0.016
Pegasus	919 $\pm$ 30	IAm	5.0 x 2.7	13.2	0.066
Sextans A	1440$\pm$ 110	IBm	5.9 x 4.9	11.9	0.044
Sextans B	1345$\pm$ 100	ImIV-V	5.1 x 3.5	11.8	0.032
WLM	932 $\pm$ 33	IB(s)m	11.5 x 4.0	10.9	0.037
NGC6822	466 $\pm$ 27	IB(s)m	15.5 x 13.5	9.3	0.236
M31	785 $\pm$ 25	SA(s)b I-II	190 x 60	3.4	0.067
M33	809 $\pm$ 24	SA(s)cd	70.8 x 41.7	5.7	0.042

[a]from the Schlegel et al. (1998) maps

was used to study in detail the resolved stellar population of 67 selected SF sites across eight galaxies, listed in Table 1. We present some of the results obtained so far. This program is a typical example of how a pathfinder survey mission such as GALEX (e.g. Bianchi 2011, Martin 2011) opens the way to follow-up programs with large telescopes from the ground and large-class space telescopes such as HST, and in the future WSO (Shustov et al. 2009, 2011).

2 GALEX Ultraviolet wide-field imaging to map SF sites

GALEX wide-field (1.2° diameter) imaging, in two Ultraviolet (UV) bands, FUV (λ_{eff}=1539Å, $\Delta\lambda$ = 1344 - 1786Å) and NUV (λ_{eff}=2316Å, $\Delta\lambda$ = 1771 - 2831Å), with a resolution of 4.2/5.3″ (FUV/NUV, Morrissey et al. 2007), is used to detect the young hot stellar populations across LG galaxies.

FUV imaging in particular offers the best sensitivity to define SF sites, unconfused by sky background or foreground Milky Way stars, and by the galaxy older, diffuse stellar populations, both relatively unconspicuous in FUV. We define contours of SF sites using background-subtracted FUV images of the whole galaxy, and measure FUV and NUV integrated fluxes by summing the flux within each contour in the original images and subtracting a locally estimated background. See Kang et al. (2009, also Fig. 2), Efremova et al. (2011), Bianchi et al. (2011) for details of the method. Here we recall only that the most sensitive parameters in such procedure are the threshold for defining the SF-sites contours, and the background subtraction. Both are especially critical in the case of dwarf galaxies, since the SF sites cover a large part of the galaxy (Figure 3) and the contrast between SF-sites and underlying main galaxy can be much higher than in the disk galaxies (Bianchi et al. 2011). The threshold is usually set at 3σ level, in order to have an objective definition of the SF regions relative to a local background. In the dwarfs with strong SF, this parameter requires individual tuning (Bianchi et al. 2011).

Out of all FUV sources detected above the threshold, we then restrict the analysis to SF sites larger than a given size, in order to avoid foreground stars, but also single stars or very small complexes in the target galaxy. This restriction ensures that only coeval regions containing a reasonable minimum number of O-type stars, hence a fully sampled IMF over the mass spectrum, are analyzed with SSP models (single burst), so the results are not affected by stochasticity of the IMF sampling. On the other hand, the selection eliminates small stellar groups, isolated stars (field), and diffuse UV emission from the galaxy, which must be measured and analyzed in a different way.

By comparing the photometry of each SF complex with SSP model colors (Bianchi 2011), we derive its age from the FUV-NUV color, and its mass from the extinction-corrected UV fluxes, the known distance, and the age. A critical step is accounting for interstellar reddening, by estimating amount and type of extinction (Bianchi, 2011). This is done for each SF site using photometry of the hot massive stars it contains. For large galaxies, like M31 and M33, the ground-based surveys of Massey et al. (2006) were initially used, that cover a large portion of the galaxies; however, optical colors are saturated at the $T_{\rm eff}$ of the hottest stars, and therefore yield uncertain results given typical photometric errors (e.g. Bianchi 2007, 2011). Moreover, ground-based imaging with typical seeing does not resolve close multiple objects, and the cores of compact stellar associations. For these reasons, we imaged with HST a sample of SF sites in these galaxies, as described below.

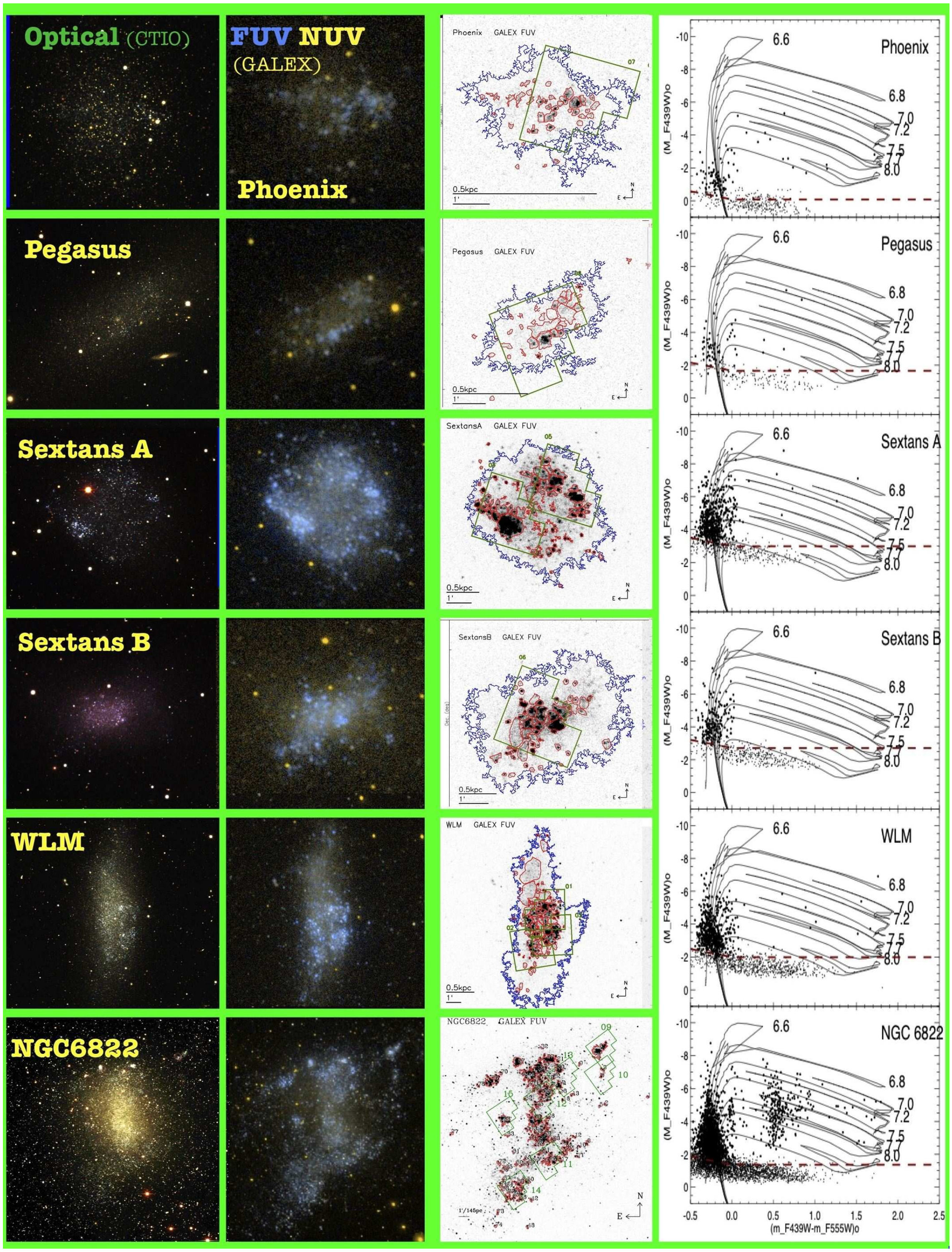

Fig. 1 The Local Group dwarf galaxies sample. Columns from left to right: (1) CTIO color-composite image (from Massey et al. 2007 survey); (2) GALEX FUV (blue) and NUV (yellow) composite image on the same scale (the yellow dots are bright cool foreground stars, which have no FUV emission); (3) SF sites (red contours) defined from GALEX FUV (gray background image), and HST images footprints (green); (4) CMD from HST photometry in WFPC2 filters equivalent to B, B-V. Absolute magnitudes are derived by applying the distances given in Table 1 and an individually-derived reddening correction for the stars with good photometry (larger dots) in several filters so that SED-fitting is possible (Fig. 4), and an average $E_{(B-V)}$ value for the rest. The red dashed line shows the completeness limit of the photometry. Note the much higher contamination by foreground stars (seen around B-V$\sim$1) towards the low latitude galaxy NGC 6822. The paucity of stars in Phoenix and Pegasus reflects their overall intrinsic faintness, and small area: only one WFPC2 pointing was used on these galaxies and on Sextans B, while two pointings were taken in Sextans A, three in WLM, and seven in NGC 6822. Isochrones (from Padua models, Girardi et al. 2002) are shown on the CMD, with log age [Myrs] labeled.

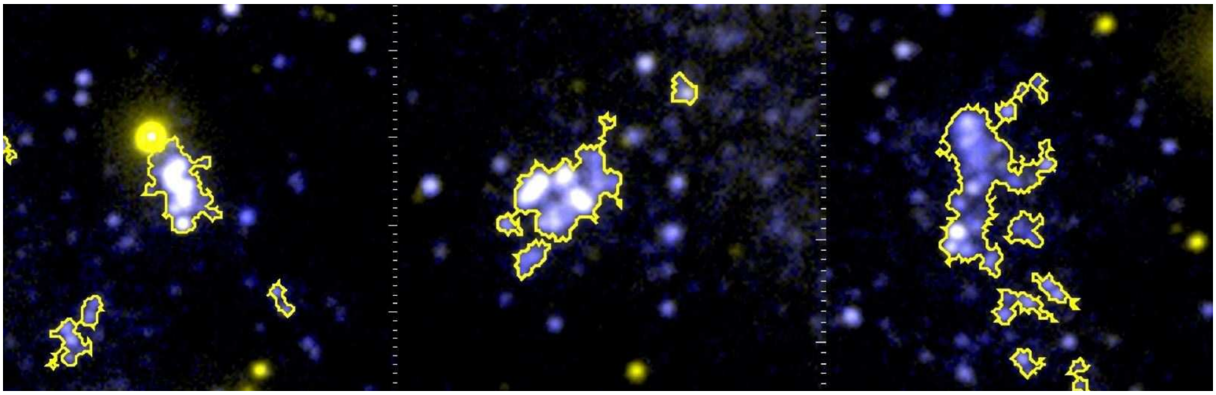

Fig. 2 Star-forming sites in M31 defined from GALEX FUV imaging by Kang et al. (2009): source contours are plotted in yellow over color-composite GALEX image cut-outs (FUV: blue, NUV: yellow). About 900 such regions were defined, over a disk with semi-major axis of 26 kpc (for comparison, the recent ground-based survey by Massey et al. (2006) extends to 17kpc)

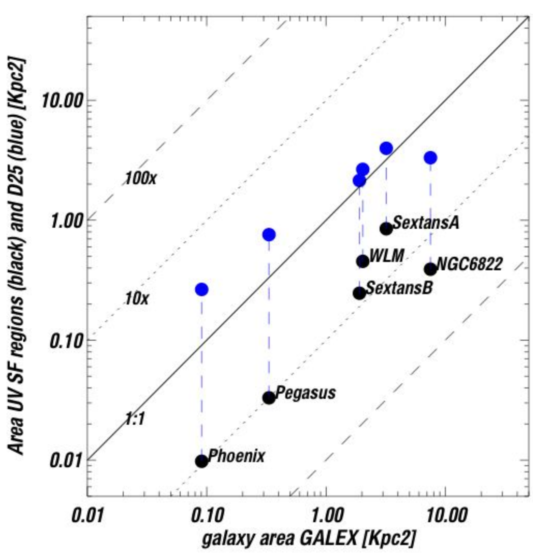

Fig. 3 The total area of the SF sites defined from FUV imaging (Section 2, red contours in Fig. 1 column 3) - black dots, and the optical D_{25} area, obtained from the distances and diameters compiled in Table 1 (blue dots), are plotted *vs* the total area of the dwarf galaxies as measured from the GALEX FUV image (blue contours in Fig. 1). Dotted and dashed lines mark factors of 10× and 100× respectively, from the 1:1 relation. M31 and M33 are off the scale in this plot: in these galaxies the SF regions amount to only a few percent of the total disk area

3 HST imaging of SF sites

We performed six-band (far-UV to near-IR) imaging with HST's WFPC2 of 67 SF sites selected from GALEX FUV imaging (previous section), for a total of over 800 HST exposures. The resulting HST photometry in far-UV (F170W), near-UV (F255W), U (F336W), B (F436W), V (F555W) and I (F814W), enables the best possible photometric characterization of the massive stars, and derivation of their physical parameters (Fig.s 4 and 5). First, UV colors increase the sensitivity to the $T_{\rm eff}$ of the hottest stars, whose optical colors are saturated (Bianchi 2007, 2011). Second, HST's spatial resolution (from 0.2 pc in Phoenix and NGC 6822 to ∼0.7 pc in Sextans A), eliminates or greatly alleviates the incidence of unresolved stars in compact SF clusters.

Fig. 1 (column 3) shows the footprints of HST imaging for the dwarf galaxies; the rest of the pointings were spent on M31 and M33, sampling differing environments and galactocentric distances. For the small galaxies, the HST fields cover almost entirely the most conspicuous and FUV-bright SF sites. In NGC 6822, some of the major OB associations were studies with previous imaging (Bianchi et al. 2001, Bianchi & Efremova 2006), and seven new fields were imaged with this program. Color-magnitude diagrams from the HST photometry (Figure 1, rightmost column) shows that hot stars content and interstellar extinction largely vary across the sample.

The exposure times in the HST filters were tuned such to obtain even S/N for the hottest stars across the whole wavelength range. For stars detected in several filters, we can derive stellar $T_{\rm eff}$ and interstellar extinction $E_{(B-V)}$ by analyzing the HST photometry with stellar model colors, constructed in the filters'

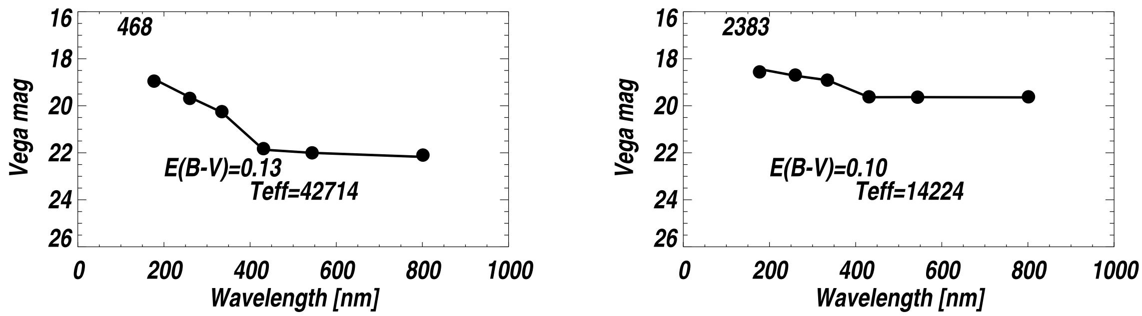

Fig. 4 HST photometry (dots) for two sample stars in Sextans A, with best-fit model (model magnitudes connected by a line). Photometric errors are smaller than the dots. The magnitudes are plotted at the λ_{eff} of each filter. The two examples span a range of $T_{\rm eff}$ in which stars have good photometry in all bands, in our HST treasury program. Reddening is derived concurrently with stellar $T_{\rm eff}$, in the SED-fitting analysis. Stellar Radius and $L_{\rm bol}$ are also derived given the known distance of the parent galaxy

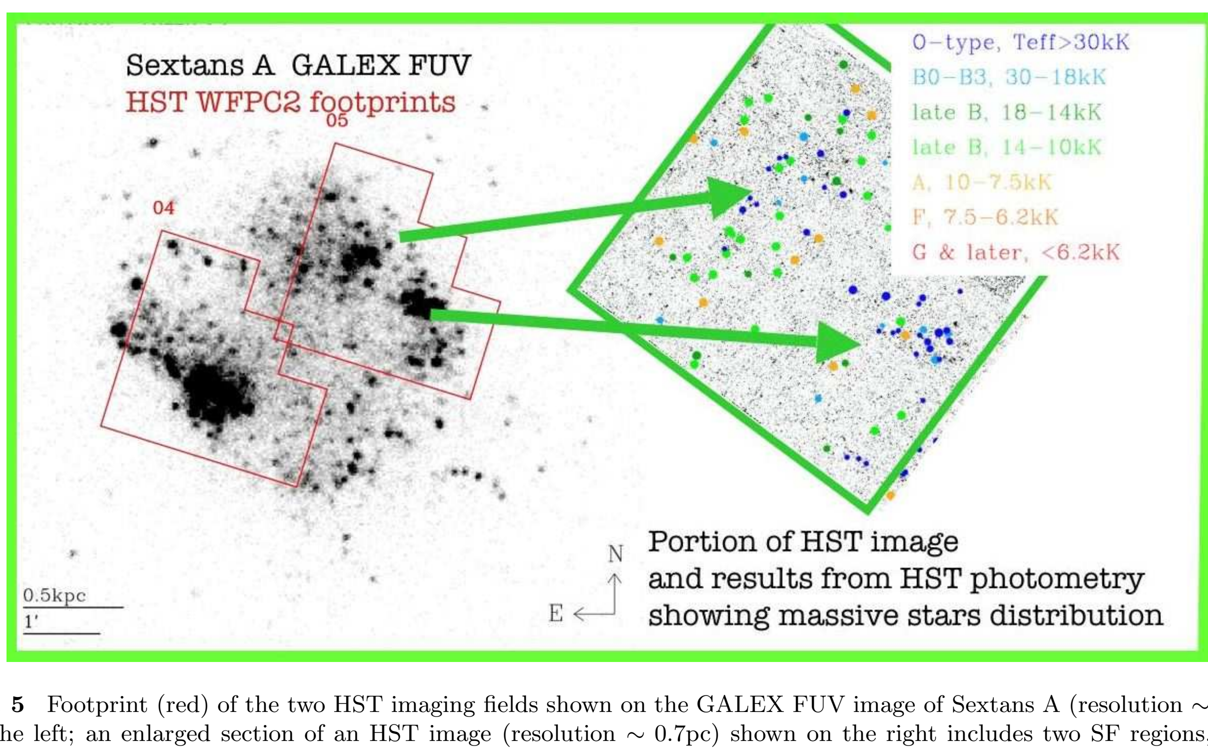

Fig. 5 Footprint (red) of the two HST imaging fields shown on the GALEX FUV image of Sextans A (resolution ∼30pc) on the left; an enlarged section of an HST image (resolution ∼ 0.7pc) shown on the right includes two SF regions, with stars color-coded according to their $T_{\rm eff}$ (estimated from the HST photometry, see Fig. 4): blue dots mark the hottest stars, green dots the ∼B types, etc. Symbol size indicates the derived stellar radius

passbands from grids of model spectra (Bianchi 2011), reddened with varying amounts and types of extinction. Selective extinction A_λ by interstellar dust is particularly severe at UV wavelengths, and more so in starburst environments. While a detailed derivation of the extinction curve $A_\lambda/E_{(B-V)}$ in each studied environment would require extensive optical and UV spectroscopy, the overall results from SED-fitting of the HST photometry qualitatively suggest an extinction steeply rising in UV in the SF sites of our sample dwarfs. Another parameter which strongly influences the results from stellar SED analysis, as well as from integrated GALEX measurements of the SF sites, is the adopted metallicity. The uncertainty that reddening corrections and metallicity assumptions bear on the results is discussed in the next section.

4 The fuel, the trigger, the smoke

The small sample of dwarf galaxies shown in this paper displays a large range of massive stars content, and of SF (Fig. 1). GALEX UV imaging provides a clear picture of where the SF is occurring, and its intensity, even in NGC6822 where foreground Galactic reddening is severe and the internal dust very patchy (Efremova et al. 2011). Hα imaging traces a fraction of these SF sites, namely the youngest and most compact ones. We derive age and stellar mass from the reddening-corrected FUV and NUV integrated phootmetry of all SF sites defined from GALEX FUV imaging, having ages up to a few hundred Myrs. By adding the masses of individual SF regions within given age ranges, we can then estimate the average star-formation rate (SFR) in these time intervals in each galaxy (as in Kang et al. 2009 for M31, Efremova et al. 2011 for NGC6822). In the dwarf galaxies' SF sites, the interstellar dust may be more starburst-like than the typical Milky Way dust, therefore we compare results obtained by assuming three differing types of dust (known from Milky Way and Magellanic Clouds environments) in Figure 6, and, because the metallicity is also uncertain, for solar and subsolar metallicities.

In Figure 6 the UV-derived SFR per unit area Σ_{SFR} is plotted *vs* the surface density of gas, taken from current literature, because the gas content gives some measure of the raw material reservoir (the fuel) available for forming stars, when triggered by internal or external dynamics inducing star formation. Therefore, is it interesting to compare stellar mass formed with gas density, a topic largely investigated in current literature (e.g. Bigiel et al. 2008, Leroy et al. 2008). While there are great uncertainties in using an average gas surface density which depends on the assumed distance, and the assumed size of the galaxy (in some cases the optical size and appearance significantly differ at other wavelengths), Kennicutt (1998) and many others have noted a robust correlation between gas density and SFR, for disk galaxies. Several authors have subsequently reported a departure from this relationship for dwarf galaxies, their SFR being lower than the "Schmidt law" (e.g. Wyder et al. 2009, Roychowdhury et al. 2009). Our results in Figure 6 appear to confirm this deviation, and in the same sense as noted by other authors; however, we would like to remark that the main message we want to convey with this figure is the very large uncertainty that the extinction correction brings in these calculations. The extinction for our sample in particular will be further constrained with follow up spectroscopy, and with more detailed

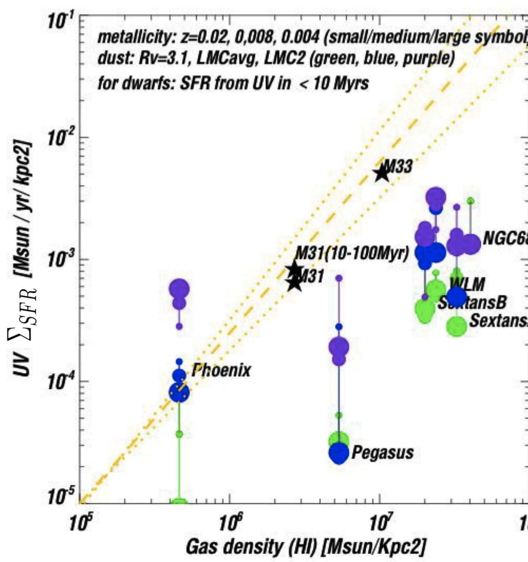

Fig. 6 The average SFR per unit area Σ_{SFR} over the past ~10Myrs derived from the GALEX integrated measurements of SF sites, *vs* gas surface density (obtained from the gas mass reported in literature, divided by the canonical D_{25} area: note that such value may therefore be an upper limit to the actual gas density). In the case of the dwarfs, such comparison shows that a large fraction of the observed HI reservoir is simply unrelated to the SF activity currently traced by the UV emission (see also Fig. 7); more importantly, this figure shows that the results strongly depend on the assumed metallicity and type of dust (see also Bianchi 2011). In this plot, we show results obtained using the MW extinction curve from Cardelli et al. (1989) (labeled "R_V=3.1"), the average LMC extinction curve outside the LMC2 starburst region (label "LMCavg") by Gordon & Clayton (1998), and the "LMC2" extinction curve by Misselt et al. (1999). The Kennicutt-Schmidt "law" and its uncertainties (in the formulation by Roychowdhury et al. 2009), which was defined for disk galaxies, is shown with yellow dashed lines.

analysis (in progress). Regarding the different stellar-mass − gas-density relation for dwarf galaxies with respect to star-forming disk galaxies, debated by several authors, we stress here another big *caveat*, illustrated by Figure 7: the distribution of the neutral hydrogen emitting at 21cm in some galaxies is completely unrelated (or even anti-correlated) with the location of the FUV-bright stellar populations (as may be expected, due to the intense UV radiation and mechanical feedback from supernova explosions and stellar winds), and may largely differ from the optical extent and appearance of the galaxy. This suggest that, for such galaxy types at least, it may be more appropriate to explore other relations, for example Σ_{SFR} *vs* molecular gas density.

Acknowledgements L.B., B.E., P.H., P.M. and K.O. acknowledge partial support from NASA grant HST-GO-11079 through STScI. GALEX (Galaxy Evolution Explorer) is a NASA Small Explorer, launched in April 2003. We gratefully acknowledge NASA's support for construction, operation, and science analysis of the GALEX mission, developed in cooperation with the Centre National d'Etudes Spatiales of France and the Korean Ministry of Science and Technology. We are very grateful to these colleagues for kindly providing their HI data, which were used to make Fig. 7: Lisa Young for HI data of Pegasus and Phoenix, Amanda Kepley for WLM, and Erwin de Blok for NGC6822

References

Bianchi, L. 2011, Astrophys. Space Sci., in press (this book)
Bianchi, L. et al. 2011, in preparation
Bianchi, L. 2009, Astrophys. Space Sci., 320, 11
Bianchi, L. 2007, in "UV Astronomy: Stars from Birth to Death", eds. A. Gomez de Castro & M. Barstow, ISBN 978-84-7491-852-6, p. 65
Bianchi, L., & Efremova, B. V. 2006, AJ, 132, 378
Bianchi,L., et al. 2001, Astron. J., 121, 2020
Bigiel, F. et al. 2008, Astron. J., 136, 2846
Cardelli,J.A. et al. 1989,Astrophys. J., 345, 245
Efremova, B., Bianchi, L, Thilker, D., et al. 2011, Astrophys. J., in press (astro-ph 1101.6051)
Girardi, L. Bertelli, G., Bressan, A. et al. 2002, Astron. Astrophys., 391, 195
Gordon, K. & Clayton, G. 1998, Astrophys. J., 500, 816
Kang, Y.-B., Bianchi, L. & Rey, S.-C. 2009, Astrophys. J., 703, 614
Kennicutt, R. 1998, Astrophys. J., 498, 541
Lee, J. et al. 2009, Astrophys. J., 706, 599
Leroy et al. 2008, Astron. J., 136, 2782
Martin, D.C. 2011, Astrophys. Space Sci., in press (this book)
Massey, P. et al. 2007, Astron. J., 133, 2393
Massey, P. et al. 2006, Astron. J., 131, 2478
Misselt, K.A. et al. 1999, Astrophys. J., 515, 128
Morrissey, P. et al. 2007, Astrophys. J. Suppl. Ser., 173, 682
Roychowdhury,S. et al. 2009, Mon. Not. R. Astron. Soc., 397, 1435
Schlegel, D. J., et al. 1998, Astrophys. J., 500, 525
Shustov, B., Sachkov, M., Gomez de Castro, A.I., et al. 2009, Astrophys. Space Sci., 320, 187
Shustov, B., Sachkov, M., Gomez de Castro, A.I., et al. 2011,Astrophys. Space Sci., in press (this book)
Wyder, T. et al. 2009, Astrophys. J., 696, 1834

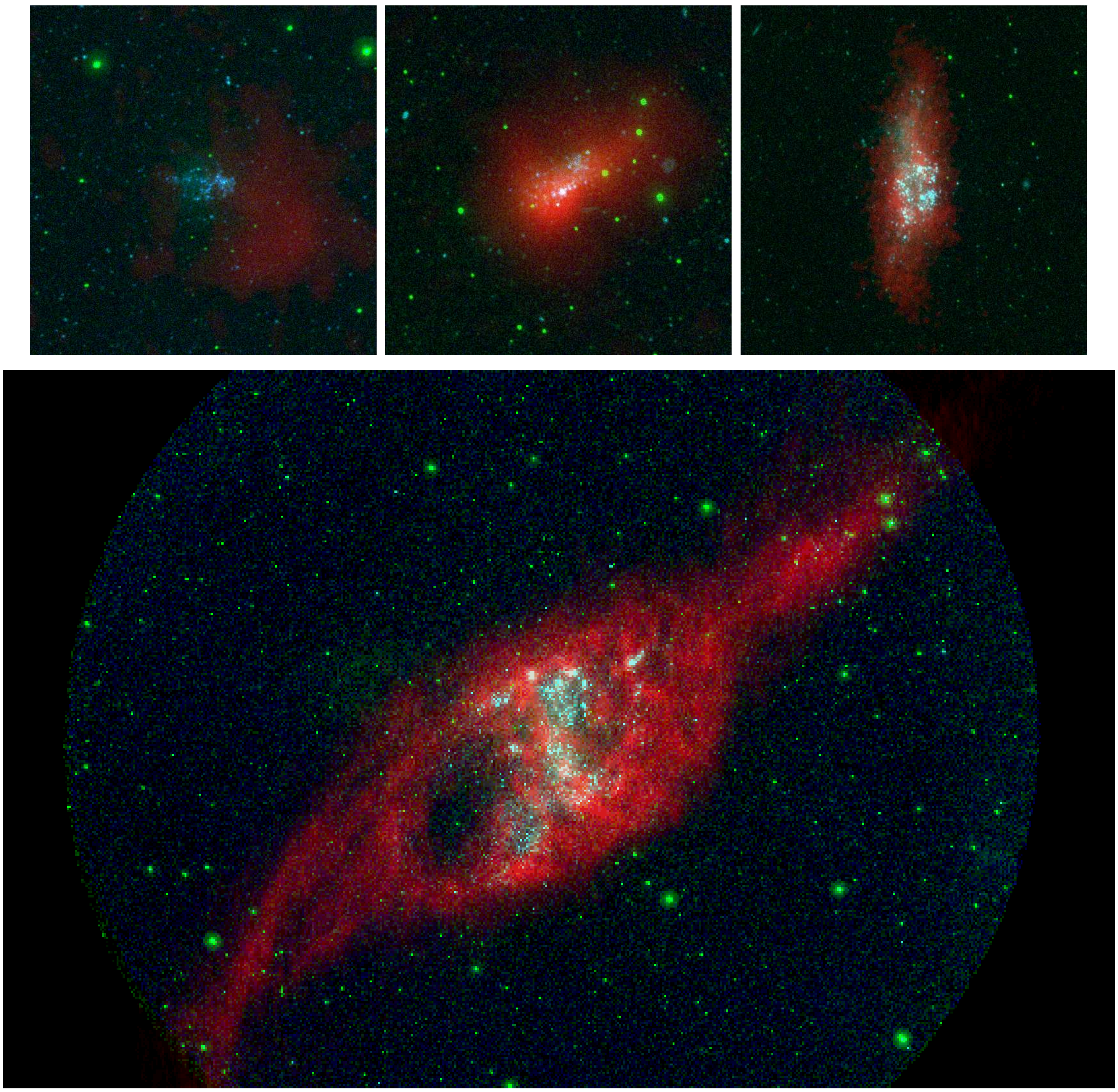

Fig. 7 Four sample dwarf galaxies shown in FUV (blue), NUV(green) and HI (red). From upper-left clockwise: Phoenix, Pegasus, WLM and NGC6822. Similarly to the 24μ dust emission, HI emission does not correlate with the intense UV emission from young massive stars. In WLM and Pegasus the neutral hydrogen emission is generally following the optical and UV shape of the galaxy, while in Phoenix the gas seems mostly removed from it. NGC6822 has an intricate shape suggesting it may be on its way to form a bar, and that - although currently isolated - it may have been dynamically less quiet in the past